catalysts

MDPI

Review

Recent Developments and Perspectives of Cobalt Sulfide-Based Composite Materials in Photocatalysis

Hui-Qi Chen, Jin-Ge Hao, Yu Wei, Wei-Ya Huang, Jia-Lin Zhang, Tao Deng, Kai Yang and Kang-Qiang Lu *

Jiangxi Provincial Key Laboratory of Functional Molecular Materials Chemistry, School of Chemistry and Chemical Engineering, Jiangxi University of Science and Technology, Ganzhou 341000, China
* Correspondence: kqlu@jxust.edu.cn

Abstract: Photocatalysis, as an inexpensive and safe technology to convert solar energy, is essential for the efficient utilization of sustainable renewable energy sources. Earth-abundant cobalt sulfide-based composites have generated great interest in the field of solar fuel conversion because of their cheap, diverse structures and facile preparation. Over the past 10 years, the number of reports on cobalt sulfide-based photocatalysts has increased year by year, and more than 500 publications on the application of cobalt sulfide groups in photocatalysis can be found in the last three years. In this review, we initially summarize the four common strategies for preparing cobalt sulfide-based composite materials. Then, the multiple roles of cobalt sulfide-based cocatalysts in photocatalysis have been discussed. After that, we present the latest progress of cobalt sulfide in four fields of photocatalysis application, including photocatalytic hydrogen production, carbon dioxide reduction, nitrogen fixation, and photocatalytic degradation of pollutants. Finally, the development prospects and challenges of cobalt sulfide-based photocatalysts are discussed. This review is expected to provide useful reference for the construction of high-performance cobalt sulfide-based composite photocatalytic materials for sustainable solar-chemical energy conversion.

Keywords: photocatalysis; cobalt sulfide; synthesis strategies; multiple roles; energy conversion

Citation: Chen, H.-Q.; Hao, J.-G.; Wei, Y.; Huang, W.-Y.; Zhang, J.-L.; Deng, T.; Yang, K.; Lu, K.-Q. Recent Developments and Perspectives of Cobalt Sulfide-Based Composite Materials in Photocatalysis. *Catalysts* **2023**, *13*, 544. https://doi.org/10.3390/catal13030544

Academic Editor: Weilin Dai

Received: 6 February 2023
Revised: 2 March 2023
Accepted: 6 March 2023
Published: 8 March 2023

1. Introduction

Energy has been the primary driving force behind civilization throughout human history. At the moment, the heavy reliance on fossil fuels has led to severe global problems such as an energy crisis and pollution of the environment [1,2]. Photocatalytic technology is an effective approach for the photochemical conversion and storage of solar energy [3–7]. Over the past 20 years, exploring new photocatalyst materials and their reaction mechanisms has been a top priority [8,9]. A complete photocatalytic reaction includes the following three steps: (i) light absorption; (ii) separation and migration of the photogenerated charges; and (iii) surface reduction and oxidation reactions [10,11]. Various photocatalysts, such as metal-free [12], metal oxides [13], metal sulfides [14], metal phosphides [15], and metal selenides [16], have been extensively studied in previous reports. However, most single-component photocatalysts have shown unsatisfactory photocatalytic activity due to weak spectral absorption, fast recombination of the photogenerated charge carrier, and an insufficient active site.

To address these problems, loading suitable cocatalysts is considered an effective way to facilitate photocatalytic reactions. Nowadays, many precious metals have been developed as cocatalysts, such as gold, platinum, and palladium [17,18]. In spite of this, the scarcity and expensiveness of these noble metals severely restrict their use on a large scale. In recent years, transition metal cocatalysts have received much attention in the field of photocatalysis due to their advantages of low cost, an abundance resources, good stability, and high catalytic activity. Especially, noble-metal-free cobalt sulfide (Co_xS_y)

has been widely explored for substituting the noble metal cocatalyst due to its sufficient catalytic sites, multivalent states, and diverse structures [19–22]. Furthermore, several excellent papers have discussed the work of cobalt sulfide-based cocatalysts in enhancing the photocatalytic properties. For example, Zhu et al. have reported a novel study on the application of cobalt sulfide-modified graphite carbon nitride for photocatalytic hydrogen evolution [23]. Cobalt sulfide acts as a cocatalyst to promote the migration of excited electrons from graphite carbon nitride to cobalt sulfide. In addition, Xu et al. also investigated the photocatalytic properties of Co_3S_4/Ag_2S nanocomposite, and the photocatalytic performance of binary nanomaterials was higher than that of a single catalyst structure [24]. In addition, Kokilavani et al. have proposed a facile chemical precipitation method for the synthesis of CoS/Ag_2WO_4 photocatalyst, and the composites show excellent performance for photocatalytic degradation and antibacterial activity [25].

Although the application of cobalt-based photocatalysts has been reviewed in the previous literature [26], there are few specific reviews that systematically summarize the synthesis, multifaceted roles, and various applications of cobalt sulfide-based composite photocatalytic materials. Therefore, it is necessary to conduct a comprehensive review of the current research progress of cobalt sulfide-based composite photocatalysts to expand their practical applications. As shown in Figure 1, in this review, we have elaborated on the synthesis methods of the cobalt sulfide-based composites. Then, the roles of cobalt sulfide-based cocatalysts in photocatalysis have been discussed. Furthermore, recent advances of the cobalt sulfide-based composite photocatalysts in photocatalytic H_2 production, CO_2 reduction, nitrogen fixation, and pollutant degradation are also reviewed. Finally, we put forward the unsolved problems and possible future development directions of cobalt sulfide-based composites in a variety of photocatalytic applications. It is hoped that this review could provide useful information for rationally designing high-performance cobalt sulfide-based composite photocatalysts.

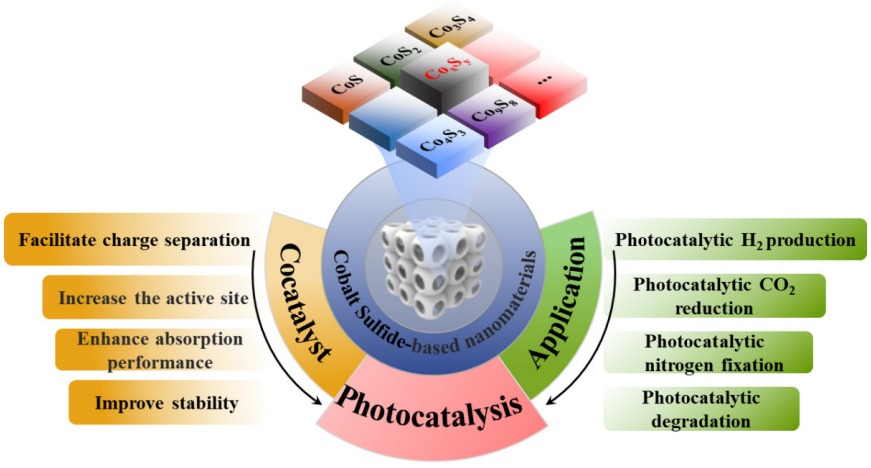

Figure 1. Schematic illustration of multifarious roles and applications of Co_xS_y in heterogeneous photocatalysis.

2. Synthesis of Cobalt Sulfide-Based Composite Material

The photocatalytic activity of cobalt sulfide-based photocatalysts mainly depends upon their size, morphology, specific surface area, and crystal structure [27,28]. Up to now, various phase and morphological cobalt sulfide-based species have been synthesized for photocatalysts. Here, in this section, we focus on the strategies for the synthesis of cobalt sulfide-based hybrid materials.

2.1. Wet Chemistry Method

For the synthesis of cobalt sulfide-based composite photocatalysts, wet chemistry has proven to be an effective technique with thioacetamide (TAA) and thiourea (TU)

as S sources [29,30]. Briefly, the vulcanization of different cobalt precursors (such as cobalt chloride or cobalt nitrate) could be achieved by using thioacetamide or thiourea in hot organic solvents at inert temperatures. In most cases, this method can be used to synthesize uniformly sized cobalt sulfide-based composite photocatalysts. As mentioned in the previously reported literatures, cobalt sulfide-based catalysis topography is mainly controlled by the S/Co ratio, solvent selection, and reaction conditions. For example, Qian et al. have synthesized Co_3S_4 by using cobalt nitrate and thioacetamide as cobalt and sulfur sources [31]. As shown in Figure 2a, Co_3S_4 showed a hollow dodecahedral structure with an average particle size of about 800 nm. In addition, the temperature has an obvious effect on the catalyst morphology. For instance, Qiu et al. have used the same cobalt-based precursor material and thiourea but different heating temperature. However, as shown in Figure 2b, a flower-like morphology of Co_3S_4 has been obtained [32]. As shown in Figure 2c,d, the flower-like morphology of Co_3S_4 can also package MoS_2 to build a nuclear-shell heterojunction photocatalyst, which shows excellent performance in the photocatalytic degradation pollutant. When constructing cobalt sulfide-based composites with specific morphology, structure, and size, it is advantageous to use wet chemistry methods, and thus wet chemistry synthesis is more common than gas-solid synthesis in the syntheses of cobalt sulfide-based composite photocatalysts [33].

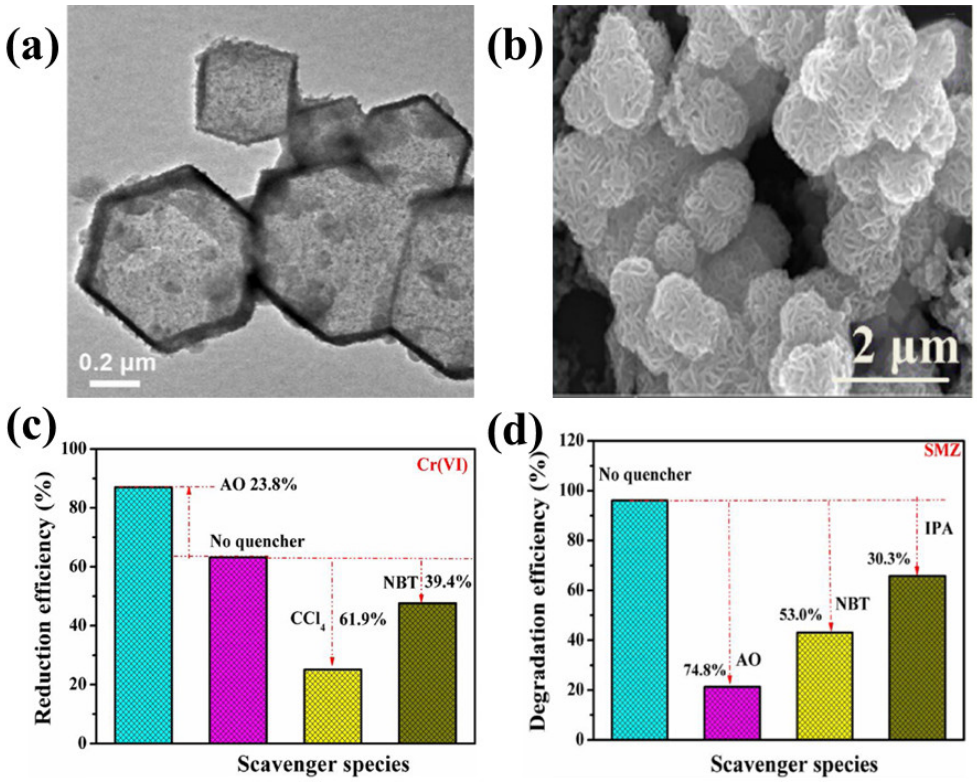

Figure 2. (**a**) TEM image of Co_3S_4. Reprinted with permission from ref. [31]. Copyright 2022, Elsevier. (**b**) SEM image of Co_3S_4. (**c**,**d**) Active species trapping experiments for (**c**) reduction of Cr(VI) and (**d**) degradation of SMZ. Reprinted with permission from ref. [32]. Copyright 2020 Elsevier.

2.2. Gas-Solid Method

Although wet chemistry techniques can produce cobalt sulfide with well-defined nanostructures, the complicated processes and low yields prevent their widespread applications [34]. Recently, the gas-solid synthesis of cobalt sulfide has attracted a wide range of attention. For the gas-solid method, sulfur powder and the cobalt-based precursor are placed in two boats of porcelain, respectively, with sulfur powder located upstream of the furnace. Following that, the samples are heated in a static atmosphere at a prescribed temperature. At temperatures over 450 °C, sulfur powder decomposes to release H_2S, which

reacts with cobalt-based precursors to form cobalt sulfide. Under certain temperatures, this surfactant-free method allows the morphology of the precursors to be preserved well, which makes it more applicable for developing different 3D self-standing cobalt sulfides with different structures [35]. For example, Xie and his collaborators synthesized the Graphdiyne-CoS_2 heterojunction nanocomposites by placing the Co(OH)F/CC composite in the tubular furnace at 500 °C [36]. Moreover, as shown in Figure 3b, Wang et al. have reported the synthesis of cobalt sulfide with multi-shell nanobox morphology by annealing the cobalt-based MOF precursor at 350 °C [37]. Cobalt sulfide with different shell numbers can be obtained by adjusting the number of shells in the cobalt-based MOF precursor, and the performance of three-layer shells is the best.

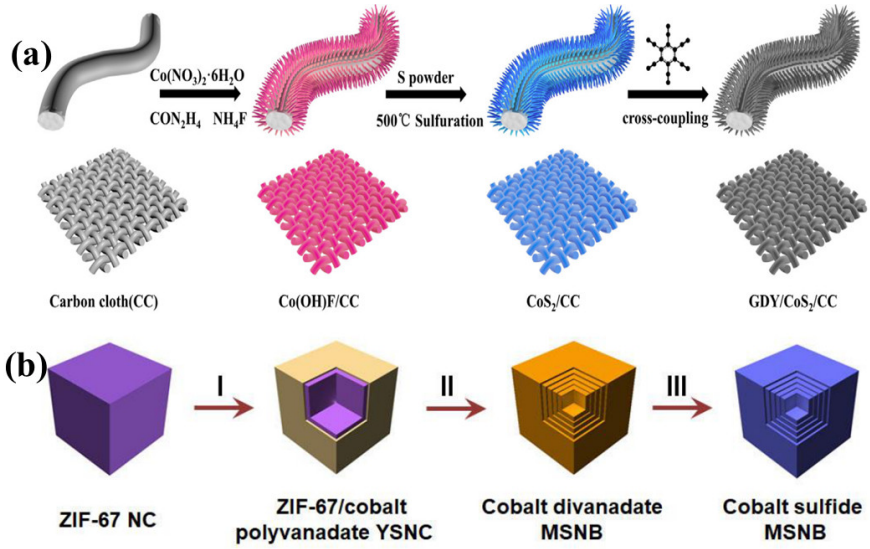

Figure 3. (**a**) A schematic diagram of the phase synthesis of GDY/CoS_2/CC catalyst. Reprinted with permission from ref. [36]. Copyright 2021, Elsevier. (**b**) A schematic illustration of the formation process of cobalt sulfide MSNB. Reprinted with permission from ref. [37]. Copyright 2019, Wiley.

2.3. Photo-Deposition Method

In many reports, the photo-deposition-assisted cocatalysts have higher catalytic performance than conventional methods because photo-deposition can promote the deposition of cocatalysts on semiconductors with well-matched positions and provide greater contact area and more active sites, thereby accelerating interfacial charge separation between the semiconductor and the co-catalysts [38,39]. The photo-deposition method was applied to deposit CoS_2 nanoparticles on g-C_3N_4 as reported by Yang et al. [38]. Appropriately sized CoS_2 nanoparticles have high adsorption and photocatalytic hydrogen production performances. The experimental results further show that the electron aggregation ability of the cocatalyst is based on the size effect of CoS_2, and the appropriate size of the cocatalyst can effectively promote the separation of photogenerated electron-hole pairs. Due to its simple and time-saving operation and good photocatalytic activity, the photo-deposition method can be used to realize the development of new non-noble metal photocatalytic materials. Moreover, amorphous cobalt sulfide obtained by the photo-deposition method has been used as an effective cocatalyst for photocatalytic water decomposition properties. For example, as exhibited in Figure 4a, Chen et al. have successfully loaded amorphous CoS_x nanodot cocatalyst onto rGO nanosheets through the photo-deposition strategies [40]. Incorporation of amorphous cobalt sulfide nanodot can significantly improve the catalytic activity of rGO/TiO_2 photocatalysts based on the formation of new active sites (Figure 4b,c). Compared to the crystalline phase, the amorphous CoS_x structure can effectively inhibit electron-hole recombination and provide a large number of active sites, exhibiting higher hydrogen production activity, thus accelerating the transfer of electrons and improving the surface H_2 precipitation rate.

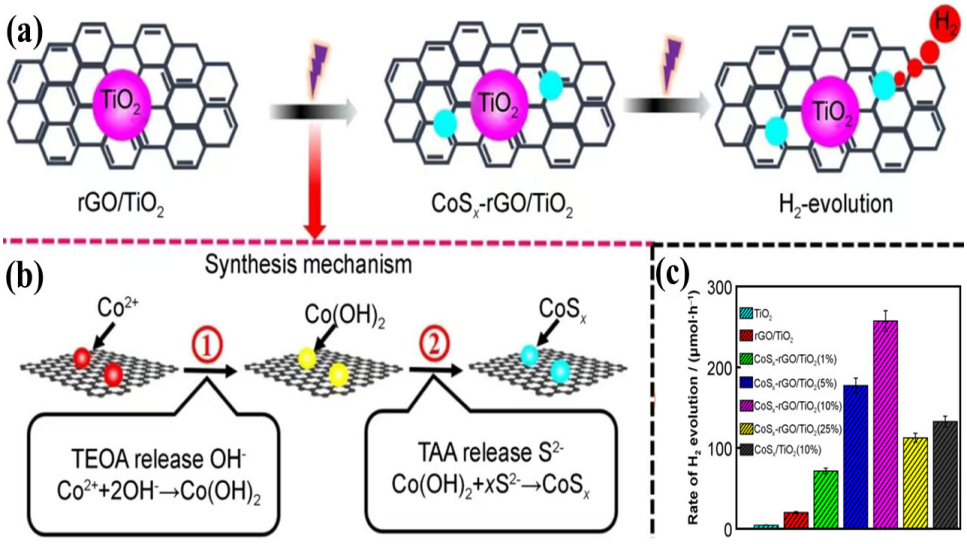

Figure 4. (**a**) Graphical illustration for synthetic process of CoS_x-rGO/TiO_2. (**b**) Formation mechanism of CoS_x on rGO surface. (**c**) H_2-production rate of TiO_2, rGO/TiO_2, CoS_x-rGO/TiO_2 (1%), CoS_x-rGO/TiO_2 (5%), CoS_x-rGO/TiO_2 (10%), CoS_x-rGO/TiO_2 (25%), and CoS_x/TiO_2 (10%). Reprinted with permission from ref. [40]. Copyright, 2021 Springer Nature.

2.4. Electrochemical Reaction Method

Several electrochemical methods, including pulse electrochemical reduction and anodic oxidation, have been reported for the synthesis of cobalt sulfide-based cocatalysts. As demonstrated in Figure 5, a facile and inexpensive one-step anodization method has been developed by Bian et al. to synthesize cobalt sulfide (CoS_x) nanosheets with mesoporous structures [41]. This porous, reverse-porous, self-grown nanostructure provides high surface-active sites for catalytic reactions and facilitates electron transfer between active materials, exhibiting excellent hydrogen evolution (HER) and oxygen evolution (OER) performances. In addition, Kubendhiran et al. synthesized the cobalt sulfide/reduced graphene oxide (CoS/rGO) nanohybrid using a single-step electrochemical method. The obtained CoS/rGO nanocomplexes show excellent selectivity and catalytic activity for H_2O_2 [42].

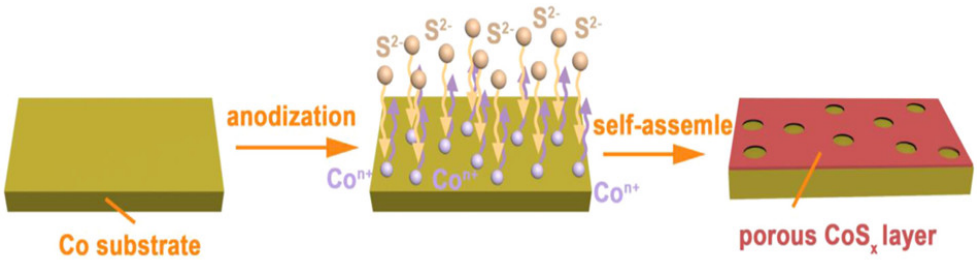

Figure 5. Schematic illustration of the anodization process of CoS_x on the metal substrate. Reprinted with permission from ref. [41]. Copyright, 2021 Elsevier.

2.5. Other Methods

In addition to the several most commonly used methods mentioned above, chemical vapor deposition (CVD) [43], microwave-assisted methods [44,45], and template-assisted methods [46] have also been used to prepare cobalt sulfide-based hybrid materials. The CVD method often requires a cumbersome manufacturing process or expensive equipment, and the prepared cobalt sulfide-based composites have poor water solubility. Therefore, CVD methods are rarely used to synthesize cobalt sulfide-based composite photocatalysts. In addition, compared with the traditional hydrothermal method, the microwave method can significantly shorten the reaction time. For instance, Souleymen et al. have synthesized

graphene-based cobalt sulfide freestanding sheets with microwave assistance [45]. The CoS_x non-layered and freestanding nanosheets were formed and exhibited higher catalytic activity due to their thin thickness, large surface area, and abundant pores compared with layered nanosheets. In addition, although the template method can prepare a cobalt sulfide-based composite photocatalyst with uniform morphology, this method requires additional removal of the template, which will increase the time and cost of the synthesis required.

3. Roles of Cobalt Sulfide-Based Cocatalysts in Photocatalysis

In general, the overall activity of photocatalytic reactions depends on the kinetic and thermodynamic synergy among strong light absorption capacity, charge separation rate, and surface reactivity. The interfacial chemical reaction is a key step in the process of photocatalytic reaction, which mainly involves charge transfer and redox reactions at the interface, which directly affect the efficiency of photocatalytic reaction [3,41]. Obviously, it is necessary to ensure that a large number of long-lived carriers participate in the surface reaction in order to increase the reaction rate [5]. Therefore, loading highly efficient co-catalysts on the semiconductor surface is an effective strategy to delay the recombination reaction and prolong the carrier lifetime. Cobalt sulfide-based cocatalysts, as one of the most important cocatalysts, have four critical roles in promoting the efficiency of photocatalytic reactions.

First of all, the incorporation of cobalt sulfide-based cocatalysts can facilitate the efficient separation of photoinduced carriers [6,47]. Once the cobalt sulfide-based cocatalysts are loaded on photocatalysts, numerous junctions will form due to the distinction in work function. These junctions are highly efficient contact forms between cobalt sulfide-based cocatalysts and host semiconductors, which can transfer photoexcited charges from photocatalysts to cocatalysts, thereby enabling the smooth completion of photocatalytic reactions.

Secondly, cobalt sulfide-based cocatalysts can offer adequate active sites for semiconductor photocatalysts, thereby enhancing the photocatalytic reaction potency [36]. The active sites are where the catalytic reaction proceeds and usually have low overpotential and an energy barrier for the catalytic reaction. These positions are more favorable to the catalytic reaction than other positions on the catalyst.

Thirdly, cobalt sulfide-based cocatalysts are helpful to improve the optical absorption performance of semiconductor photocatalysts [30,47]. The adsorption and activation of protons are the crucial links for enhancing the potency of the photocatalyst in the process of photocatalytic hydrogen production [30]. Cobalt sulfide with a narrow bandgap can enhance the optical absorption ability of photocatalysts by stimulating the absorption of light with a wide wavelength. In addition, cobalt sulfide can also be directly formed into a hollow structure or nanosheet array structure, which increases the specific surface area of the photocatalyst and reduces the diffusion distance of the photogenerated carrier to improve the absorption efficiency of the semiconductor.

Fourthly, the loading of cobalt sulfide-based cocatalysts can inhibit the photocorrosion of some semiconductors and enhance the stability of the photocatalysts [48]. When the cobalt sulfide-based cocatalyst with good photocatalytic activity and stability is anchored to the semiconductor, the surface reaction will be carried out on the cobalt sulfide cocatalyst, thus improving the efficiency of the photocatalytic reaction [49].

4. Cobalt Sulfide-Based Composite Material for Photocatalysis

4.1. Photocatalytic H_2 Production

Recently, semiconductor photocatalytic water decomposition has been improved by integrating appropriate co-catalysts. Due to the sufficient catalytic site and easy preparation, cobalt sulfide-based cocatalysts have been widely applied as co-catalysts for various semiconductors toward photocatalytic hydrogen evolution [50–53]. Fu et al. have illustrated that combining a hollow cobalt sulfide (CoS_x) polyhedral cocatalyst with g-C_3N_4 can effectively accelerate the separation of photoinduced charges in g-C_3N_4 and provide an abundant active site to promote redox reactions (Figure 6a) [54]. In addition, as shown in

Figure 6b, the hollow structure of the CoS_x polyhedron can also allow multiple reflections of light to enhance the light collection of g-C_3N_4. Thus, the photocatalytic performance of the 2% CoS_x/g-C_3N_4 hybrids was significantly better than that of the blank g-C_3N_4. Obviously, the incorporation of cobalt sulfide could act as a cocatalyst to accelerate the separation and transfer of photo-generated electron-hole pairs and reduce the overpotential of the hydrogen production reaction. Qiu et al. reported that CdS nanorods loaded with CoS_2 nanoparticles exhibited excellent photocatalytic hydrogen production activity, which was 13 times higher than that of pristine CdS NRs samples, and the optimized CoS_2/CdS NRs photocatalyst had high stability and recyclability [55].

In addition to the cobalt sulfide single component cocatalyst, multicomponent co-catalysts exhibit superior co-catalytic activity than single component cocatalysts. For example, Li et al. have reported an excellent composite photocatalyst by combining CoS with $Co(OH)_2$ on g-C_3N_4 to construct a dual cocatalyst [56]. The photocatalytic hydrogen production rate of the CoS/Co $(OH)_2$/g-C_3N_4 composite photocatalyst is 311 times higher than that of pure g-C_3N_4, which is due to the synergistic effect of the dual cocatalysts. In the dual cocatalyst system, CoS cocatalyst acts as an electron acceptor to facilitate the separation of photogenerated carriers, and $Co(OH)_2$ can also act as a conductor to diffuse photon-generated electrons. Moreover, in addition to acting as a co-catalyst, cobalt sulfide has also been reported as a semiconductor for H_2 production. For example, Zhang et al. used a simple hydrothermal synthesis method to in situ grow two-dimensional $ZnIn_2S_4$ on one-dimensional hollow Co_9S_8 nanotubes to form a Co_9S_8/$ZnIn_2S_4$ heterostructure [57]. As shown in Figure 6c, type-I heterostructures are constructed when the Co_9S_8 nanotubes are covered with $ZnIn_2S_4$ nanosheets. When the Co_9S_8/$ZnIn_2S_4$ composites are excited to generate electron-hole pairs, the photogenerated electrons can migrate rapidly from the CB of $ZnIn_2S_4$ to that of Co_9S_8. Consequently, the Co_9S_8/$ZnIn_2S_4$ heterostructure achieves a higher photocatalytic activity than pure $ZnIn_2S_4$. Apart from the aforementioned research, Table 1 summarizes other studies that have employed cobalt sulfide-based semiconductor composites for photocatalytic H_2 production.

Table 1. Cobalt sulfide-based semiconductor composites for photocatalytic H_2 production.

Cocatalysts	Semiconductor	Light Source (Sacrificial Reagent)	Photocatalytic Activity ($\mu mol \cdot g^{-1} \cdot h^{-1}$)	Ref.
CoS_2	CdS	$\lambda \geq 400$ nm (Lactic acid or Na_2S/Na_2SO_3)	58,100	[58]
Co_3S_4/Co@C	CdS	$\lambda > 420$ nm (Na_2S and Na_2SO_3)	15,170	[30]
Co_4S_3	CdS	$\lambda \geq 420$ nm (Lactic acid)	12,360	[59]
CdS/Co_9S_8	RGO	$\lambda > 420$ nm (Na_2S and Na_2SO_3)	4820	[49]
Co_9S_8	$ZnIn_2S_4$	$\lambda > 420$ nm (TEOA)	6250	[60]
CoS_2	$Zn_{0.5}Cd_{0.5}S$	$\lambda \geq 420$ nm (L-lactic acid)	25,150	[48]
CoS_2	ZnS	$\lambda > 420$ nm (Na_2S and Na_2SO_3)	8001	[35]
Co_3S_4	g-C_3N_4	$\lambda \geq 400$ nm (TEOA)	20,536.4	[61]
CoS	TiO_2	$\lambda \geq 400$ nm (Lactic acid)	1945	[47]
Co_4S_3/CNFs	$CdIn_2S_4$	$\lambda > 420$ nm (Lactic acid)	25,870	[62]
Co_3S_4	g-C_3N_4	$\lambda > 420$ nm (TEOA)	2120	[63]

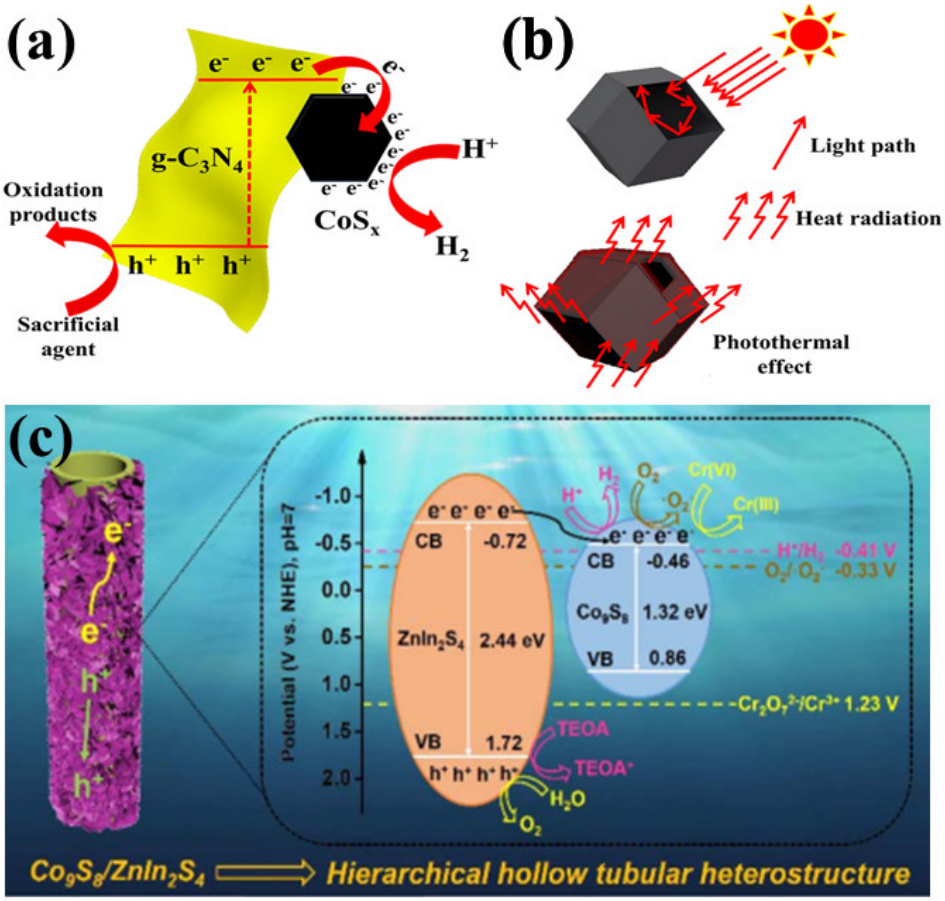

Figure 6. (**a**) Potential mechanism for photocatalytic H_2 evolution on $CoS_x/g-C_3N_4$ composite photocatalyst. (**b**) Schemes for light path and photothermal effects within the hollow CoS_x polyhedron. Reprinted with permission from ref. [54]. Copyright 2018, American Chemical Society. (**c**) Schematic illustration of the fabrication process of hierarchical $Co_9S_8/ZnIn_2S_4$ tubular photocatalysts. Reprinted with permission from ref. [57]. Copyright 2020, Wiley.

4.2. Photocatalytic CO_2 Reduction

In addition to being used as a cocatalyst for photocatalytic H_2 production, cobalt sulfide can also be used as efficient photocatalytic for CO_2 reduction [64,65]. For example, Zhang et al. have composited the hollow Co_9S_8 nanocages with $ZnIn_2S_4$ nanosheets and CdS quantum dots to construct a ternary composite photocatalyst [29]. As shown in Figure 7a, the hollow structure of Co_9S_8 nanocages promotes multiple reflections of sunlight in the cavity, which enhanced the light absorption of $ZnIn_2S_4$ nanosheets and CdS quantum dots. In addition, as shown in Figure 7b, the ternary composite photocatalyst form a double Z-type heterojunction, which facilitates the separation and migration of photogenic electron hole pairs. Therefore, the photocatalytic performance of the Co_9S_8@$ZnIn_2S_4$/CdS hybrid is obviously better than that of blank CdS and $ZnIn_2S_4$, as described in Figure 7c.

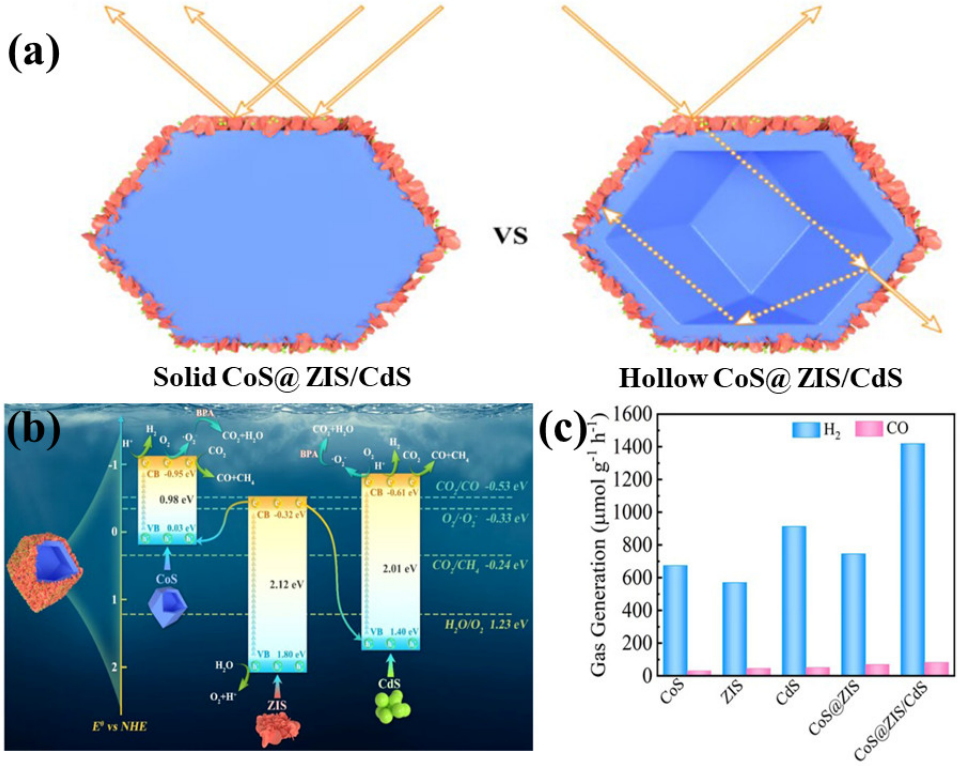

Figure 7. (**a**,**b**) Illustration of multiple reflections (**a**) and proposed photocatalytic mechanism over CoS@ZIS/CdS heterojunction (**b**). (**c**) Comparison of H_2 and CO generation over different samples. Reprinted with permission from ref. [29]. Copyright 2022, Elsevier.

Moreover, photocatalytic reduction of CO_2 to methanol is another ideal approach for solar energy conversion. Ma et al. have prepared carbon nitride (CN) loaded with cobalt sulfide (CS) as a cocatalyst. The optimized CS/CN photocatalyst was 2.3 times more selective for CH_3OH than CN [66]. It was confirmed that the introduction of cobalt sulfide can improve the selectivity of CH_3OH. The cobalt sulfide not only provides the H_2O oxidation center but also can significantly weaken the overpotential of the H_2O oxidation half reaction, thus effectively avoiding the formation of strongly oxidized radicals.

Furthermore, Wang et al. have reported hierarchical $FeCoS_2$-CoS_2 double-shelled nanotubes as a composite photocatalyst for CO_2 reduction [67]. As shown in Figure 8a, $FeCoS_2$-CoS_2 composites can be obtained after ion-exchange reactions and sulfidation reactions with MIL-88A as precursors. As shown in Figure 8b, $FeCoS_2$-CoS_2 composites present a uniform hierarchical nanosheet structure. When the $Ru(bpy)_3^{2+}$ is used as the photosensitizer, the optimal $FeCoS_2$-CoS_2 composite shows excellent photocatalytic activity with a CO generation rate of 28.1 μmol h^{-1}, which is better than the individuals of $FeCoS_2$ and CoS_2 and their physical mixtures sample (Figure 8c). As illustrated in Figure 8d, the unique hierarchical nanosheet structure reduces diffusion length and enhances scattering in the cavity, which inhibits electron-hole recombination and exposes active sites for redox reactions, thus improving the photocatalytic activity of the $FeCoS_2$-CoS_2 composite.

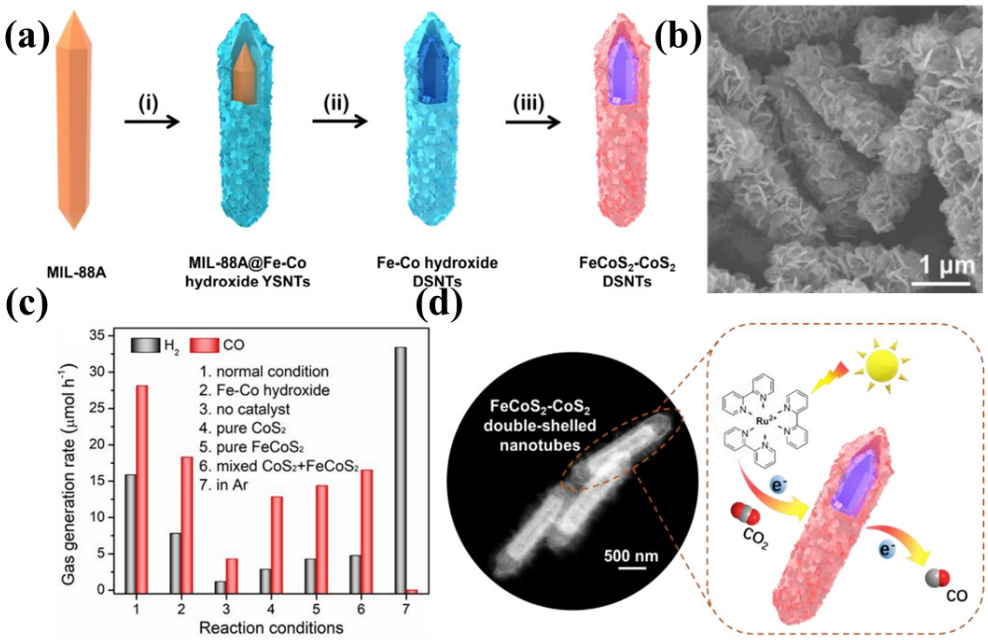

Figure 8. (**a**) Illustration of the synthetic process for hierarchical $FeCoS_2-CoS_2$. (**b**) FESEM images of one $FeCoS_2-CoS_2$. (**c**) Photoreduction of CO_2 under different reaction conditions. (**d**) Schematic diagram of CO_2 photoreduction over $FeCoS_2$-CoS_2. Reprinted with permission from ref. [67]. Copyright 2020, Wiley.

4.3. Photocatalytic Nitrogen Fixation

Neither humans nor the earth's ecosystem can survive without the ability to synthesize ammonia [68]. The production of this foundation sustaining life on earth is based on both industrial and biological fixation levels of 200×10^6 tons per year [69]. At present, nitrogen fixation is principally carried out in three ways: (i) biological nitrogen fixation. Some micro-organisms, such as nitrogen-fixing bacteria, use their own nitrogenase to fix N_2 molecules for biological nitrogen fixation; (ii) high-energy nitrogen fixation in geochemical processes, such as lightning; (iii) the energy-intensive Haber–Bosch method for industrial nitrogen fixation. However, biological and geochemical nitrogen fixation solely account for a tiny fraction of the fixed nitrogen supply. The Haber–Bosch process, which uses N_2 and H_2 as sources and iron-based compounds as the main material, is currently the main route for the synthesis of industrial ammonia. Nevertheless, this process requires a great deal of energy input while generating large emissions of by-products (such as carbon dioxide), which may cause environmental hazards. Hence, developing high-selectivity photocatalysts for nitrogen-reducing ammonia is challenging and interesting research [69]. Recently, Yuan et al. have demonstrated that loading Ru/CoS_x to g-C_3N_4 nanosheets can effectively activate N_2 molecules and facilitate the separation of light-induced electron-hole pairs in g-C_3N_4 [70]. As shown in Figure 9a, in comparison with pure CN, Ru-Vs-CoS/CN shows obviously enhanced photocatalytic activity, reaching 1.28% apparent quantum efficiency at 400 nm and 0.042% solar-to-ammonia efficiency. The excellent nitrogen reduction reaction performance is attributed to the fact that the sulfur vacancies in CoS_x can effectively promote the selective chemisorption of N_2 molecules. In addition, an N_2 molecule is bridged against the side-on Ru-Co center by the undercoordination of Ru and Co atoms at the Ru/CoS_x interface. Furthermore, as shown in Figure 9b, the plasmonic Ru/CoS_x interface enhances light absorption to generate energetic charge-carriers, accelerates charge separation and transfer, and therefore kinetically facilitates the fixation of N_2. This confirms that the presence of vacancies on the surface of cobalt sulfide-based nanomaterials exhibits excellent photocatalytic NRR performance, as it can modify the electronic structure, decrease the coordination number of surface atoms, facilitate the formation of dangling bonds, and greatly promote the formation of N_2 chemisorption

and activation. The N_2-fixation mechanism outlined in Figure 9c indicates the hydrogen evolution reaction (HER) on Ru occurs easily due to its good free energy of hydrogen production (−0.07 eV). Meanwhile, the active hydrogen adsorption on Co and desorption on S limit the hydrogen evolution reaction (HER) on Ru.

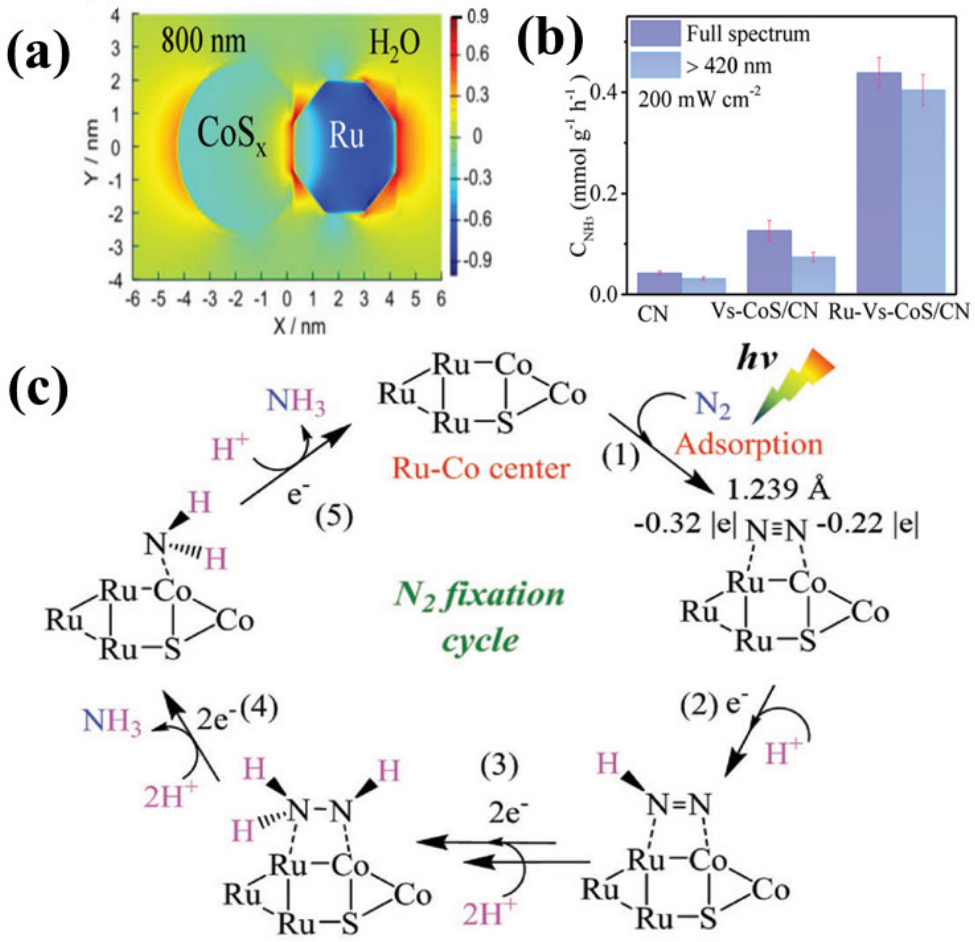

Figure 9. (**a**) Photocatalytic NH_3 production rates over different samples (**b**) FDTD electric field distribution observed from the *z*-axis (parallel to incident light) at Ru/CoS_x nanoparticles (800 nm irradiation). (**c**) Proposed photocatalytic N_2RR pathway on Ru−Vs−CoS/CN. Reprinted with permission from ref. [70]. Copyright 2020, Wiley.

4.4. Photocatalytic Degradation

Recent research shows that cobalt sulfide-based materials, such as CoS, CoS_2, and Co_3S_4, are important candidate catalysts for photocatalytic organic pollutants degradation [71–74]. For instance, $Co_{2.67}S_4$ shows excellent photocatalytic degradation efficiency of methylene blue (MB) under UV, visible, and near-infrared irradiation [75]. As shown in Figure 10a, the valence state change of cobalt ions effectively separates electrons from holes and accelerates electron transfer, thus enhancing the activity of photocatalytic degradation. In addition to single cobalt-based sulfide materials, cobalt sulfide, as a co-catalyst, can be combined with host semiconductors for photocatalytic degradation. For example, Tang et al. have designed a two-dimensional CoS/BiOBr heterojunction, which shows a 5.3-fold higher degradation rate as compared to pure BiOBr (Figure 10b) [76]. As shown in Figure 10c,d, when the BiOBr and the CoS combine to construct the CoS/BiOBr heterojunction photocatalyst, the electrons on the CB of the CoS can be easily transferred to the CB of the BiOBr. In addition, the VB of BiOBr can oxidize glyphosate directly, producing small molecules or ions (PO_4^{3-}, etc.). Simultaneously, some holes also migrate from BiOBr to

CoS, leading to effective photogenerated charge carrier separation and thereby boosting the photocatalytic performance of the CoS/BiOBr composite.

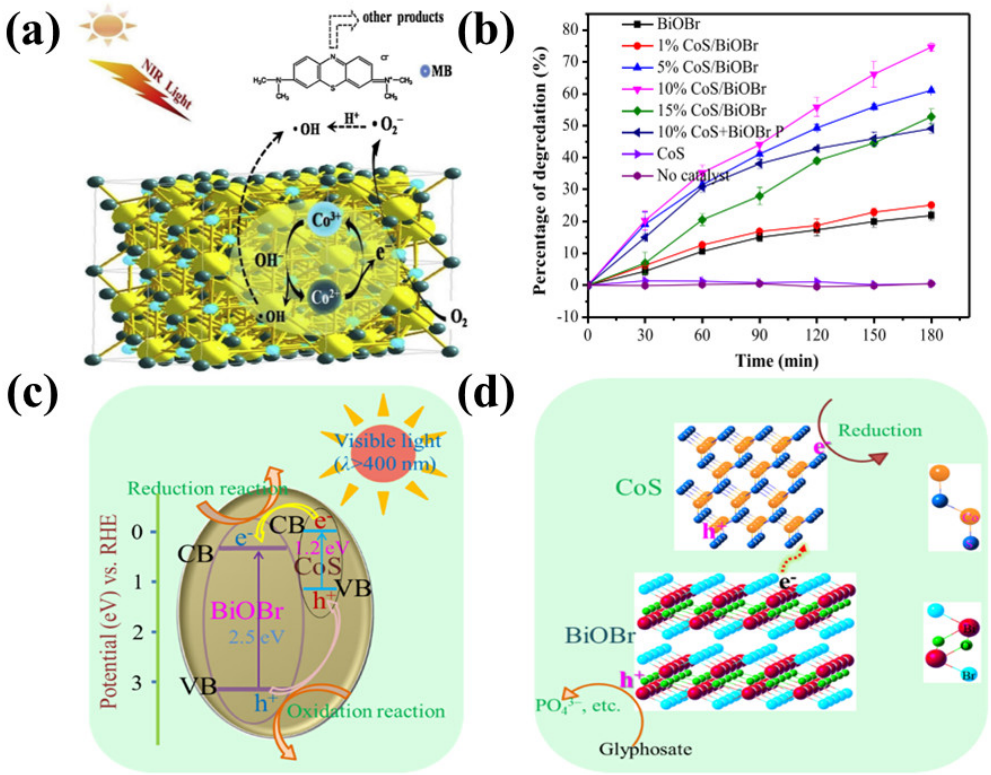

Figure 10. (**a**) Illustrative diagram of the $Co_{2.67}S_4$ system under NIR light irradiation. Copyright 2017, Elsevier. (**b**) Photocatalytic degradation of glyphosate. (**c**) A schematic illustration of the photogenerated carrier transfer process and (**d**) photocatalytic degradation process over CoS/BiOBr. Reprinted with permission from ref. [76]. Copyright 2021, Elsevier.

Moreover, Zhang et al. have covered uniformly MoS_2 nanosheets on CoS_2 nanoparticles to construct CoS_2/MoS_2-nitrogen-doped graphene aerogels for photocatalytic organic pollutants degradation [77]. When MoS_2 is combined with CoS_2, the band gap of MoS_2 can be narrowed and the optical response range can be expanded. At the same time, CoS_2 can effectively accelerate the charge separation and increase the surface-active sites. Taking advantage of these advantages, the optimized three-dimensional CoS_2/MoS_2-nitrogen-doped graphene aerogel photocatalyst can degrade pollutants up to 97.1% within 60 minimums and still maintain 95.1% after three cycles. Apart from the aforementioned research, Table 2 summarizes other studies that have employed cobalt sulfide-based composites for photocatalytic organic pollutant degradation.

Table 2. Cobalt sulfide-based semiconductor composites for photocatalytic degradation.

Catalysts	Conditions	Catalyst Amount (mg)	Dye/Concentration	%Degradation/Time (min)	Ref.
Pg-C_3N_4 /Co_3O_4/CoS)	different pH (pH = 3, 5, 7, 9, 11) 500 W Xe lamp	5	BPF/30 mg·L^{-1}	99/50	[72]
CoS-TEA	300 W Xe lamp	20	RhB/10 mg·L^{-1}	97.34/80	[78]
CoS-rGO	pH = 5, sunlight with light intensity of ~680 W/m	5	CR/10 mg·mL^{-1}	88.03/40	[79]

Table 2. *Cont.*

Catalysts	Conditions	Catalyst Amount (mg)	Dye/Concentration	%Degradation/Time (min)	Ref.
CoS-rGO/PMS	different operating conditions at room temperature	25	RhB/14 mg·L^{-1}	95/8	[80]
Co_3S_4-SnO_2/PVPCS	25 W UV lamp (UV lamp: 5.5 cm, and light intensity: at 3.0 mW·cm^{-2})	10	LDC/10 mg·mL^{-1}	98.72/30	[81]
CoS NS	Neutral pH, 200 W tungsten lamp	5	MB/20 mg·L^{-1} RhB/20 mg·L^{-1} CV/20 mg·L^{-1} NB/20 mg·L^{-1}	99.8/10 99.5/45 99.4/3 99.8/5	[82]
CdS/N-CoS_x	300 W Xe lamp	10	Cr(VI)/10 mg·mL^{-1}	100/25	[83]
Graphite/Cobalt Sulfide/PANI composite	Magnetic Agitation under dark and Visible light (15 watt)	25	CR/25 mg·mL^{-1}	99.55/120	[84]
CoS_2-CeO_2/CSCS	under UV light irradiation	20	4NP/10 mg·L^{-1}	95.42/60	[85]

5. Conclusions and Perspectives

In this review, we have summarized recent progress in cobalt sulfide syntheses, especially morphological and temperature-dependent design guidelines, and their applications in photocatalytic hydrogen production, CO_2 reduction, nitrogen fixation, and degradation pollutant. In spite of the significant progress made to date, some challenges and opportunities for further advancement in this research field are presented as follows:

(1) Nowadays, cobalt sulfide is regarded as an inexpensive, easily synthesized, and efficient photocatalyst. However, cobalt sulfide is much less stable than the catalysts required for practical applications. Therefore, more efforts need to be made to enhance the stability of cobalt sulfide;

(2) To date, there are almost no practical synthetic methods for cobalt sulfide-based composites that are available for mass production to meet real-life applications. Therefore, the development of industrial-scale production methods with stable, efficient, and low-cost cobalt sulfide-based composites is significant;

(3) Since sacrificial agents are inevitably used for current photocatalytic reactions, this causes serious problem of increased reaction costs and waste of reaction energy. In addition, the enhancement of photocatalytic activity is mainly determined by the consumption degree and survival time of its photosynthetic holes or electrons. In this regard, the combination of H_2 production, the reduction of CO_2, and N_2 fixation with oxidative organic synthesis in a photosynthetic reaction is a feasible method for avoiding the use of sacrificial agents;

(4) Many problems still need to be addressed in further development. For example, studies on the active sites, and charge carrier dynamics of cobalt sulfide catalysts are still in their infancy. In addition, the mechanism of cobalt sulfide as a photocatalytic catalyst also deserves further investigation. Therefore, it is very necessary to conduct more thorough and systematic studies of these problems, both theoretically and experimentally. Notably, in situ characterization techniques are capable of detecting the change of structure within the cobalt sulfide group in real time, which requires more effort to develop.

Author Contributions: Conceptualization, H.-Q.C. and K.-Q.L.; software, J.-G.H., Y.W. and K.Y.; formal analysis, W.-Y.H., J.-L.Z. and T.D.; resources, K.Y., W.-Y.H. and K.-Q.L.; data curation, H.-Q.C. and J.-G.H.; writing—original draft preparation, H.-Q.C.; writing—review and editing, K.-Q.L.; supervision, K.-Q.L. All authors have read and agreed to the published version of the manuscript.

Funding: This study is financially supported by Jiangxi University of Science and Technology students' innovation and entrepreneurship training program (Preparation of graphene aerogel/semiconductor composite photocatalytic materials and their performance research, 202210407022), the Jiangxi Provincial Natural Science Foundation (20212BAB213016, 20224BAB203018, 20224ACB213010, 204302600031), the Postdoctoral Research Projects of Jiangxi Province (2021RC11, 204302600031), the Jiangxi Province "Double Thousand Plan", the high-level talent research launch project of JXUST (205200100518), the National Natural Science Foundation of China (21962006), the Jiangxi Provincial Academic and Technical Leaders Training Program—Young Talents (20204BCJL23037), the Program of Qingjiang Excellent Young Talents, JXUST(JXUSTQJBJ2020005), the Ganzhou Young Talents Program of Jiangxi Province (204301000111), and the Jiangxi Provincial Key Laboratory of Functional Molecular Materials Chemistry (20212BCD42018).

Data Availability Statement: The original contributions presented in the study are included in the article; further inquiries can be directed to the corresponding author.

Conflicts of Interest: The authors declare no conflict of interest.

References

1. Li, Q.; Wang, X.P.; Xiong, X.Q.; Zhu, S.H.; Meng, Z.H.; Hong, Y.Y.; Lin, C.X.; Liu, X.Y.; Lin, Y.H. Graphene-supported biomimetic catalysts with synergistic effect of adsorption and degradation for efficient dye capture and removal. *Chin. Chem. Lett.* **2020**, *31*, 239–243. [CrossRef]
2. Yang, M.Q.; Zhang, N.; Pagliaro, M.; Xu, Y.J. Artificial photosynthesis over graphene–semiconductor composites. Are we getting better? *Chem. Soc. Rev.* **2014**, *43*, 8240–8254. [CrossRef] [PubMed]
3. Xing, Y.P.; Wang, X.K.; Hao, S.H.; Zhang, X.L.; Wang, X.; Ma, W.X.; Zhao, G.; Xu, X.J. Recent advances in the improvement of g-C_3N_4 based photocatalytic materials. *Chin. Chem. Lett.* **2021**, *32*, 13–20. [CrossRef]
4. Li, Y.H.; Tang, Z.R.; Xu, Y.J. Multifunctional graphene-based composite photocatalysts oriented by multifaced roles of graphene in photocatalysis. *Chin. J. Catal.* **2022**, *43*, 708–730. [CrossRef]
5. Xie, L.; Hao, J.G.; Chen, H.Q.; Li, Z.X.; Ge, S.Y.; Mi, Y.; Yang, K.; Lu, K.Q. Recent advances of nickel hydroxide-based cocatalysts in heterogeneous photocatalysis. *Catal. Commun.* **2022**, *162*, 106371. [CrossRef]
6. Ye, C.; Li, J.X.; Wu, H.L.; Li, X.B.; Chen, B.; Tung, C.H.; Wu, L.Z. Enhanced charge separation efficiency accelerates hydrogen evolution from water of carbon nitride and 3,4,9,10-Perylene-tetracarboxylic dianhydride composite photocatalyst. *ACS Appl. Mater. Interfaces* **2018**, *10*, 3515–3521. [CrossRef]
7. Lu, K.Q.; Li, Y.H.; Tang, Z.R.; Xu, Y.J. Roles of graphene oxide in heterogeneous photocatalysis. *ACS Mater. Au* **2021**, *1*, 37–54. [CrossRef]
8. Jamshaid, M.; Nazir, M.A.; Najam, T.; Shah, S.S.A.; Khan, H.M.; Rehman, A.U. Facile synthesis of Yb^{3+}-Zn^{2+} substituted M type hexaferrites: Structural, electric and photocatalytic properties under visible light for methylene blue removal. *Chem. Phys. Lett.* **2022**, *805*, 139939. [CrossRef]
9. Jamshaid, M.; Khan, H.M.; Nazir, M.A.; Wattoo, M.A.; Shahzad, K.; Malik, M.; Rehman, A.-U. A novel bentonite–cobalt doped bismuth ferrite nanoparticles with boosted visible light induced photodegradation of methyl orange: Synthesis, characterization and analysis of physiochemical changes. *Int. J. Environ. Anal. Chem.* **2022**. [CrossRef]
10. Tan, C.L.; Qi, M.Y.; Tang, Z.R.; Xu, Y.J. Cocatalyst decorated $ZnIn_2S_4$ composites for cooperative alcohol conversion and H_2 evolution. *Appl. Catal. B* **2021**, *298*, 120541. [CrossRef]
11. Wu, C.X.; Xing, Z.P.; Yang, S.L.; Li, Z.Z.; Zhou, W. Nanoreactors for photocatalysis. *Coordin. Chem. Rev.* **2023**, *477*, 214939. [CrossRef]
12. Rahman, M.Z.; Kibria, M.G.; Mullins, C.B. Metal-free photocatalysts for hydrogen evolution. *Chem. Soc. Rev.* **2020**, *49*, 1887–1931. [CrossRef]
13. Mohd Adnan, M.A.; Phoon, B.L.; Muhd Julkapli, N. Mitigation of pollutants by chitosan/metallic oxide photocatalyst: A review. *J. Clean. Prod.* **2020**, *261*, 121190. [CrossRef]
14. Wu, X.J.; Xie, S.J.; Zhang, H.K.; Zhang, Q.H.; Sels, B.F.; Wang, Y. Metal Sulfide Photocatalysts for Lignocellulose Valorization. *Adv. Mater.* **2021**, *33*, 2007129. [CrossRef]
15. Ma, B.J.; Zhang, R.S.; Lin, K.Y.; Liu, H.X.; Wang, X.Y.; Liu, W.Y.; Zhan, H.J. Large-scale synthesis of noble-metal-free phosphide/CdS composite photocatalysts for enhanced H_2 evolution under visible light irradiation. *Chin. J. Catal.* **2018**, *39*, 527–533. [CrossRef]
16. Sobhani, A.; Salavati Niasari, M. Transition metal selenides and diselenides: Hydrothermal fabrication, investigation of morphology, particle size and and their applications in photocatalyst. *Adv. Colloid Interface Sci.* **2021**, *287*, 102321. [CrossRef]
17. Weng, B.; Qi, M.Y.; Han, C.; Tang, Z.R.; Xu, Y.J. Photocorrosion inhibition of semiconductor-based photocatalysts: Basic principle, current development, and future perspective. *ACS Catal.* **2019**, *9*, 4642–4687. [CrossRef]
18. Wu, H.K.; Li, Y.H.; Qi, M.Y.; Lin, Q.; Xu, Y.J. Enhanced photocatalytic CO_2 reduction with suppressing H_2 evolution via Pt cocatalyst and surface SiO_2 coating. *Appl. Catal. B* **2020**, *278*, 119267. [CrossRef]

19. Yao, S.; Huang, T.Z.; Fang, H.Y.; Yu, J.M.; Meganathan, M.D.; Cui, Z.X.; Yuan, X.X. Cobalt sulfides as efficient catalyst towards oxygen reduction reactions. *Chin. Chem. Lett.* **2020**, *31*, 530–534. [CrossRef]
20. Fan, S.Q.; Wang, Y.; Li, Z.S.; Zeng, Z.; Guo, S.X.; Huang, S.Y.; Ma, X.B. Carbon layer-coated ordered mesoporous silica supported Co-based catalysts for higher alcohol synthesis: The role of carbon source. *Chin. Chem. Lett.* **2020**, *31*, 525–529. [CrossRef]
21. Ren, X.; Shi, J.Y.; Duan, R.H.; Di, J.; Xue, C.; Luo, X.; Liu, Q.; Xia, M.Y.; Lin, B.; Tang, W. Construction of high-efficiency CoS@Nb_2O_5 heterojunctions accelerating charge transfer for boosting photocatalytic hydrogen evolution. *Chin. Chem. Lett.* **2022**, *33*, 4700–4704. [CrossRef]
22. Li, J.K.; Li, M.; Jin, Z.L. Rational design of a cobalt sulfide/bismuth sulfide S-scheme heterojunction for efficient photocatalytic hydrogen evolution. *J. Colloid Interface Sci.* **2021**, *592*, 237–248. [CrossRef] [PubMed]
23. Zhu, Y.S.; Xu, Y.; Hou, Y.D.; Ding, Z.X.; Wang, X.C. Cobalt sulfide modified graphitic carbon nitride semiconductor for solar hydrogen production. *Int. J. Hydrog. Energy* **2014**, *39*, 11873–11879. [CrossRef]
24. Xu, M.Y.; Niu, H.L.; Huang, J.J.; Song, J.M.; Mao, C.J.; Zhang, S.Y.; Zhu, C.F.; Chen, C.L. Facile synthesis of graphene-like Co_3S_4 nanosheet/Ag_2S nanocomposite with enhanced performance in visible-light photocatalysis. *Appl. Surf. Sci.* **2015**, *351*, 374–381. [CrossRef]
25. Kokilavani, S.; Syed, A.; Al-Shwaiman, H.A.; Alkhulaifi, M.M.; Almajdhi, F.N.; Elgorban, A.M.; Khan, S.S. Preparation of plasmonic CoS/Ag_2WO_4 nanocomposites: Efficient visible light driven photocatalysts and enhanced anti-microbial activity. *Colloid Interface Sci. Commun.* **2021**, *42*, 100415. [CrossRef]
26. Wang, W.; Li, T.; Komarneni, S.; Lu, X.; Liu, B.J. Recent advances in Co-based co-catalysts for efficient photocatalytic hydrogen generation. *J. Colloid Interface Sci.* **2022**, *608*, 1553–1575. [CrossRef]
27. Ma, X.Y.; Zhang, W.; Deng, Y.D.; Zhong, C.; Hu, W.B.; Han, X.P. Phase and composition controlled synthesis of cobalt sulfide hollow nanospheres for electrocatalytic water splitting. *Nanoscale* **2018**, *10*, 4816–4824. [CrossRef]
28. Yin, Y.; Erdonmez, C.K.; Cabot, A.; Hughes, S.; Alivisatos, A.P. Colloidal Synthesis of Hollow Cobalt Sulfide Nanocrystals. *Adv. Funct. Mater.* **2006**, *16*, 1389–1399. [CrossRef]
29. Zhang, Y.; Wu, Y.X.; Wan, L.; Ding, H.J.; Li, H.X.; Wang, X.Y.; Zhang, W.H. Hollow core–shell Co_9S_8@$ZnIn_2S_4$/CdS nanoreactor for efficient photothermal effect and CO_2 photoelectron. *Appl. Catal. B* **2022**, *311*, 121255. [CrossRef]
30. Liu, Y.P.; Wang, B.X.; Zhang, Q.; Yang, S.Y.; Li, Y.H.; Zuo, J.L.; Wang, H.J.; Peng, F. A novel bicomponent Co_3S_4/Co@C cocatalyst on CdS, accelerating charge separation for highly efficient photocatalytic hydrogen evolution. *Green Chem.* **2020**, *22*, 238–247. [CrossRef]
31. Qian, X.Y.; Yin, Y.X.; Lu, Y.C.; Xia, J.W.; Huang, B.J.; Sun, J.W.; He, G.Y.; Chen, H.Q. Construction of sulfur vacancies enriched hollow zinc cobalt bimetallic sulfides for high-performance supercapacitors. *J. Alloys Compd.* **2022**, *913*, 165191. [CrossRef]
32. Qiu, J.L.; Zheng, W.T.; Yuan, R.R.; Yue, C.L.; Li, D.W.; Liu, F.Q.; Zhu, J.J. A novel 3D nanofibrous aerogel-based MoS_2@Co_3S_4 heterojunction photocatalyst for water remediation and hydrogen evolution under simulated solar irradiation. *Appl. Catal. B* **2020**, *264*, 118514. [CrossRef]
33. Chen, F.Y.; Yu, C.L.; Wei, L.F.; Fan, Q.Z.; Ma, F.; Zeng, J.L.; Yi, J.H.; Yang, K.; Ji, H.B. Fabrication and characterization of $ZnTiO_3$/$Zn_2Ti_3O_8$/ZnO ternary photocatalyst for synergetic removal of aqueous organic pollutants and Cr(VI) ions. *Sci. Total Environ.* **2020**, *706*, 136026. [CrossRef]
34. Hao, J.G.; Chen, H.Q.; Xie, L.; Li, Z.X.; Zhang, J.L.; Huang, W.Y.; Deng, T.; Lu, K.Q.; Yang, K. Rationally designed Sb_2S_3/PDI composites with enhanced visible light photoactivity. *Catal. Commun.* **2022**, *162*, 106368. [CrossRef]
35. Wang, B.L.; Guo, S.H.; Xin, X.; Zhang, Y.Z.; Wang, Y.J.; Li, C.H.; Song, Y.R.; Deng, D.S.; Li, X.H.; Sobrido, A.J.; et al. Heat diffusion-induced gradient energy level in multishell bisulfides for highly efficient photocatalytic hydrogen production. *Adv. Energy Mater.* **2020**, *10*, 2001575. [CrossRef]
36. Xie, W.J.; Liu, K.; Shi, G.D.; Fu, X.L.; Chen, X.J.; Fan, Z.X.; Liu, M.; Yuan, M.J.; Wang, M. CoS_2 nanowires supported graphdiyne for highly efficient hydrogen evolution reaction. *J. Energy. Chem.* **2021**, *60*, 272–278. [CrossRef]
37. Wang, X.; Chen, Y.; Fang, Y.J.; Zhang, J.T.; Gao, S.Y.; Lou, X.W. Synthesis of Cobalt Sulfide Multi-shelled Nanoboxes with Precisely Controlled Two to Five Shells for Sodium-Ion Batteries. *Angew. Chem. Int. Ed.* **2019**, *58*, 2675–2679. [CrossRef]
38. Yang, S.; Guo, X.Y.; Liu, K.; Li, Y.F.; Li, T.; Gu, X.R.; Arenal, R.; Zheng, X.X.; Li, W.; Sun, C.Z.; et al. Size effect of CoS_2 cocatalyst on photocatalytic hydrogen evolution performance of g-C_3N_4. *J. Colloid Interface Sci.* **2023**, *635*, 305–315. [CrossRef]
39. Zhao, H.; Mao, Q.Y.; Jian, L.; Dong, Y.M.; Zhu, Y.F. Photodeposition of earth-abundant cocatalysts in photocatalytic water splitting: Methods, functions, and mechanisms. *Chin. J. Catal.* **2022**, *43*, 1774–1804. [CrossRef]
40. Chen, F.; Feng, H.F.; Luo, W.; Wang, P.; Yu, H.G.; Fan, J.J. Simultaneous realization of direct photodeposition and high H_2-production activity of amorphous cobalt sulfide nanodot-modified rGO/TiO_2 photocatalyst. *Rare Met.* **2021**, *40*, 3125–3134. [CrossRef]
41. Bian, H.D.; Chen, T.Y.; Chen, Z.X.; Liu, J.H.; Li, Z.B.; Du, P.; Zhou, B.B.; Zeng, X.R.; Tang, J.N.; Liu, C. One-step synthesis of mesoporous Cobalt sulfides (CoS_x) on the metal substrate as an efficient bifunctional electrode for overall water splitting. *Electrochim. Acta* **2021**, *389*, 138786. [CrossRef]
42. Kubendhiran, S.; Thirumalraj, B.; Chen, S.M.; Karuppiah, C. Electrochemical co-preparation of cobalt sulfide/reduced graphene oxide composite for electrocatalytic activity and determination of H_2O_2 in biological samples. *J. Colloid Interface Sci.* **2018**, *509*, 153–162. [CrossRef] [PubMed]

43. Ighodalo, K.O.; Ezealigo, B.N.; Agbogu, A.; Nwanya, A.C.; Obi, D.; Mammah, S.L.; Botha, S.; Bucher, R.; Maaza, M.; Ezema, F.I. The effect of deposition cycles on intrinsic and electrochemical properties of metallic cobalt sulfide by Simple chemical route. *Mater. Sci. Semicond. Process.* **2019**, *101*, 16–27. [CrossRef]
44. Wang, F.P.; Li, G.F.; Zheng, J.F.; Ma, J.; Yang, C.X.; Wang, Q.Z. Microwave synthesis of three-dimensional nickel cobalt sulfide nanosheets grown on nickel foam for high-performance asymmetric supercapacitors. *J. Colloid Interface Sci.* **2018**, *516*, 48–56. [CrossRef] [PubMed]
45. Souleymen, R.; Wang, Z.T.; Qiao, C.; Naveed, M.; Cao, C.B. Microwave-assisted synthesis of graphene-like cobalt sulfide freestanding sheets as an efficient bifunctional electrocatalyst for overall water splitting. *J. Mater. Chem. A* **2018**, *6*, 7592–7607. [CrossRef]
46. Wang, J.; Zhong, H.X.; Wang, Z.L.; Meng, F.L.; Zhang, X.B. Integrated Three-Dimensional Carbon Paper/Carbon Tubes/Cobalt-Sulfide Sheets as an Efficient Electrode for Overall Water Splitting. *ACS Nano* **2016**, *10*, 2342–2348. [CrossRef] [PubMed]
47. Park, H.; Kim, S.; Kim, T.; Kim, Y.; Joo, S.W.; Kang, M. CoS@TiO_2 S-scheme heterojunction photocatalyst for hydrogen production from photoinduced water splitting. *J. Clean. Prod.* **2021**, *319*, 128819. [CrossRef]
48. Ma, L.J.; Xu, J.; Zhao, S.; Li, L.J.; Liu, Y. Construction of $CoS_2/Zn_{0.5}Cd_{0.5}S$ S-scheme heterojunction for enhancing H_2 evolution activity under visible light. *Chem. Eur. J.* **2021**, *27*, 15795–15805. [CrossRef]
49. Kai, S.S.; Xi, B.J.; Li, H.B.; Xiong, S.L. Z-scheme CdS/Co_9S_8-RGO for photocatalytic hydrogen production. *Inorg. Chem. Front.* **2020**, *7*, 2692–2701. [CrossRef]
50. Cheng, J.Z.; Tan, Z.R.; Xing, Y.Q.; Shen, Z.Q.; Zhang, Y.J.; Liu, L.L.; Yang, K.; Chen, L.; Liu, S.Y. Exfoliated conjugated porous polymer nanosheets for highly efficient photocatalytic hydrogen evolution. *J. Mater. Chem. A* **2021**, *9*, 5787–5795. [CrossRef]
51. Si, Y.; Lv, Z.; Lu, L.; Liu, M.; Wen, Y.; Chen, Y.; Jin, H.; Liu, J.; Song, W. Revealing important role of graphitic carbon nitride surface catalytic activity in photocatalytic hydrogen evolution by using different carbon co-catalysts. *Appl. Surf. Sci.* **2019**, *491*, 236–244. [CrossRef]
52. Zhao, C.; Li, Q.; Xie, Y.; Zhang, L.P.; Xiao, X.D.; Wang, D.; Jiao, Y.Q.; Hurd Price, C.A.; Jiang, B.J.; Liu, J. Three-dimensional assemblies of carbon nitride tubes as nanoreactors for enhanced photocatalytic hydrogen production. *J. Mater. Chem. A* **2020**, *8*, 305–312. [CrossRef]
53. Zhang, Y.Z.; Shi, J.W.; Huang, Z.X.; Guan, X.J.; Zong, S.C.; Cheng, C.; Zheng, B.T.; Guo, L.J. Synchronous construction of CoS_2 in-situ loading and S doping for g-C_3N_4: Enhanced photocatalytic H_2-evolution activity and mechanism insight. *Chem. Eng. J.* **2020**, *401*, 126135. [CrossRef]
54. Fu, J.W.; Bie, C.B.; Cheng, B.; Jiang, C.J.; Yu, J.G. Hollow CoS_x polyhedrons act as high-efficiency cocatalyst for enhancing the photocatalytic hydrogen generation of g-C_3N_4. *ACS Sustain. Chem. Eng.* **2018**, *6*, 2767–2779. [CrossRef]
55. Qiu, B.Q.; Li, C.X.; Shen, X.Q.; Wang, W.L.; Ren, H.; Li, Y.; Tang, J. Revealing the size effect of metallic CoS_2 on CdS nanorods for photocatalytic hydrogen evolution based on Schottky junction. *Appl. Catal. A Gen.* **2020**, *592*, 117377. [CrossRef]
56. Li, K.; Lin, Y.Z.; Wang, K.; Wang, Y.J.; Zhang, Y.; Zhang, Y.Z.; Liu, F.T. Rational design of cocatalyst system for improving the photocatalytic hydrogen evolution activity of graphite carbon nitride. *Appl. Catal. B* **2020**, *268*, 118402. [CrossRef]
57. Zhang, G.P.; Chen, D.Y.; Li, N.J.; Xu, Q.F.; Li, H.; He, J.H.; Lu, J.M. Construction of hierarchical hollow $Co_9S_8/ZnIn_2S_4$ tubular heterostructures for highly efficient solar energy conversion and environmental remediation. *Angew. Chem. Int. Ed.* **2020**, *59*, 8255–8261. [CrossRef]
58. Tang, J.; Gao, B.; Pan, J.B.; Chen, L.; Zhao, Z.H.; Shen, S.; Guo, J.K.; Au, C.T.; Yin, S.F. CdS nanorods anchored with CoS_2 nanoparticles for enhanced photocatalytic hydrogen production. *Appl. Catal. A Gen.* **2019**, *588*, 117281. [CrossRef]
59. Kumar, D.P.; Park, H.; Kim, E.H.; Hong, S.; Gopannagari, M.; Reddy, D.A.; Kim, T.K. Noble metal-free metal-organic framework-derived onion slice-type hollow cobalt sulfide nanostructures: Enhanced activity of CdS for improving photocatalytic hydrogen production. *Appl. Catal. B* **2018**, *224*, 230–238. [CrossRef]
60. Wang, S.B.; Guan, B.; Yuan Wang, X.; Lou, X.W.D. Formation of hierarchical Co_9S_8@$ZnIn_2S_4$ heterostructured cages as an efficient photocatalyst for hydrogen evolution. *J. Am. Chem. Soc.* **2018**, *140*, 15145–15148. [CrossRef]
61. Yang, H.C.; Yin, J.M.; Cao, R.Y.; Sun, P.X.; Zhang, S.W.; Xu, X.J. Constructing highly dispersed 0D Co_3S_4 quantum dots/2D g-C_3N_4 nanosheets nanocomposites for excellent photocatalytic performance. *Sci. Bull.* **2019**, *64*, 1510–1517. [CrossRef] [PubMed]
62. Guo, S.W.; Li, Y.K.; Xue, C.; Sun, Y.R.; Wu, C.; Shao, G.S.; Zhang, P. Controllable construction of hierarchically $CdIn_2S_4$/CNFs/Co_4S_3 nanofiber networks towards photocatalytic hydrogen evolution. *Chem. Eng. J.* **2021**, *419*, 129213. [CrossRef]
63. Wang, Y.P.; Hao, X.Q.; Zhang, L.J.; Jin, Z.L.; Zhao, T.S. Amorphous Co_3S_4 nanoparticle-modified tubular g-C_3N_4 forms step-scheme heterojunctions for photocatalytic hydrogen production. *Catal. Sci. Technol.* **2021**, *11*, 943–955. [CrossRef]
64. Yang, M.Q.; Xu, Y.J. Photocatalytic conversion of CO_2 over graphene-based composites: Current status and future perspective. *Nanoscale Horiz.* **2016**, *1*, 185–200. [CrossRef] [PubMed]
65. Ran, J.; Jaroniec, M.; Qiao, S.-Z. Cocatalysts in semiconductor-based photocatalytic CO_2 reduction: Achievements, challenges, and opportunities. *Adv. Mater.* **2018**, *30*, 1704649. [CrossRef]
66. Ma, M.; Huang, Z.; Wang, R.; Zhang, R.; Yang, T.; Rao, Z.; Fa, W.; Zhang, F.; Cao, Y.; Yu, S.; et al. Targeted H_2O activation to manipulate the selective photocatalytic reduction of CO_2 to CH_3OH over carbon nitride-supported cobalt sulfide. *Green Chem.* **2022**, *24*, 8791–8799. [CrossRef]
67. Wang, Y.; Wang, S.B.; Zhang, S.; Lin Lou, X.W. Formation of hierarchical $FeCoS_2$–CoS_2 double-shelled nanotubes with enhanced performance for photocatalytic reduction of CO_2. *Angew. Chem. Int. Ed.* **2020**, *59*, 11918–11922. [CrossRef]

68. Chen, X.; Li, J.Y.; Tang, Z.R.; Xu, Y.J. Surface-defect-engineered photocatalyst for nitrogen fixation into value-added chemical feedstocks. *Catal. Sci. Technol.* **2020**, *10*, 6098–6110. [CrossRef]
69. Chen, X.; Qi, M.Y.; Li, Y.H.; Tang, Z.R.; Xu, Y.J. Enhanced ambient ammonia photosynthesis by Mo-doped Bi_5O_7Br nanosheets with light-switchable oxygen vacancies. *Chin. J. Catal.* **2021**, *42*, 2020–2026. [CrossRef]
70. Yuan, J.L.; Yi, X.Y.; Tang, Y.H.; Liu, M.J.; Liu, C.B. Efficient photocatalytic nitrogen fixation: Enhanced polarization, activation, and cleavage by asymmetrical electron donation to N≡N bond. *Adv. Funct. Mater.* **2020**, *30*, 1906983. [CrossRef]
71. Yu, C.L.; Zeng, D.B.; Fan, Q.Z.; Yang, K.; Zeng, J.L.; Wei, L.F.; Yi, J.H.; Ji, H.B. The distinct role of boron doping in Sn_3O_4 microspheres for synergistic removal of phenols and Cr(vi) in simulated wastewater. *Environ. Sci. Nano* **2020**, *7*, 286–303. [CrossRef]
72. Guo, D.; Wang, Y.Q.; Chen, C.; He, J.Q.; Zhu, M.L.; Chen, J.; Zhang, C.L. A multi-structural carbon nitride co-modified by Co, S to dramatically enhance mineralization of Bisphenol f in the photocatalysis-PMS oxidation coupling system. *Chem. Eng. J.* **2021**, *422*, 130035. [CrossRef]
73. Sohrabnezhad, S.; Pourahmad, A.; Radaee, E. Photocatalytic degradation of basic blue 9 by CoS nanoparticles supported on AlMCM-41 material as a catalyst. *J. Hazard. Mater.* **2009**, *170*, 184–190. [CrossRef]
74. Wu, Y.Y.; Zheng, H.L.; Li, H.; Sun, Y.J.; Zhao, C.; Zhao, R.; Zhang, C. Magnetic nickel cobalt sulfide/sodium dodecyl benzene sulfonate with excellent ciprofloxacin adsorption capacity and wide pH adaptability. *Chem. Eng. J.* **2021**, *426*, 127208. [CrossRef]
75. Wu, Z.Z.; Yuan, X.Z.; Wang, H.; Wu, Z.B.; Jiang, L.B.; Wang, H.; Zhang, L.; Xiao, Z.H.; Chen, X.H.; Zeng, G.M. Facile synthesis of a novel full-spectrum-responsive $Co_{2.67}S_4$ nanoparticles for UV-, vis- and NIR-driven photocatalysis. *Appl. Catal. B* **2017**, *202*, 104–111. [CrossRef]
76. Tang, Q.Y.; Yang, M.J.; Yang, S.Y.; Xu, Y.H. Enhanced photocatalytic degradation of glyphosate over 2D CoS/BiOBr heterojunctions under visible light irradiation. *J. Hazard. Mater.* **2021**, *407*, 124798. [CrossRef]
77. Zhang, L.; Wu, L.Z.; Feng, Z.Q.; Meng, Q.; Li, Y.; Duan, T. Adopting sulfur-atom sharing strategy to construct CoS_2/MoS_2 heterostructure on three-dimensional nitrogen-doped graphene aerogels: A novel photocatalyst for wastewater treatment. *J. Environ. Chem. Eng.* **2021**, *9*, 104771. [CrossRef]
78. Yein, W.T.; Wang, Q.; Wu, J.Z.; Wu, X.H. Converting CoS-TEA hybrid compound to CoS defective ultrathin nanosheets and their enhanced photocatalytic property. *J. Mol. Liq.* **2018**, *268*, 273–283. [CrossRef]
79. Borthakur, P.; Das, M.R. Hydrothermal assisted decoration of NiS_2 and CoS nanoparticles on the reduced graphene oxide nanosheets for sunlight driven photocatalytic degradation of azo dye: Effect of background electrolyte and surface charge. *J. Colloid Interface Sci.* **2018**, *516*, 342–354. [CrossRef] [PubMed]
80. Amirache, L.; Barka-Bouaifel, F.; Borthakur, P.; Das, M.R.; Ahouari, H.; Vezin, H.; Barras, A.; Ouddane, B.; Szunerits, S.; Boukherroub, R. Cobalt sulfide-reduced graphene oxide: An efficient catalyst for the degradation of rhodamine B and pentachlorophenol using peroxymonosulfate. *J. Environ. Chem. Eng.* **2021**, *9*, 106018. [CrossRef]
81. Huang, M.; Zhang, R.; Yang, Z.R.; Chen, J.; Deng, J.; Fakhri, A.; Gupta, V.K. Synthesis of Co_3S_4-SnO_2/polyvinylpyrrolidone-cellulose heterojunction as highly performance catalyst for photocatalytic and antimicrobial properties under ultra-violet irradiation. *Int. J. Biol. Macromol.* **2020**, *162*, 220–228. [CrossRef] [PubMed]
82. Khan, A.A.; Kumari, S.; Chowdhury, A.; Hussain, S. Phase tuned originated dual properties of cobalt sulfide nanostructures as photocatalyst and adsorbent for removal of dye pollutants. *ACS Appl. Nano Mater.* **2018**, *1*, 3474–3485. [CrossRef]
83. Zhang, L.X.; Feng, L.P.; Li, P.; Chen, X.; Gao, Y.; Gong, Y.S.; Du, Z.L.; Zhang, S.; Zhang, A.C.; Chen, G.F.; et al. Plasma-assisted doping of nitrogen into cobalt sulfide for loading cadmium sulfide: A direct Z-scheme heterojunction for efficiently photocatalytic Cr(VI) reduction under visible light. *Chem. Eng. J.* **2021**, *417*, 129222. [CrossRef]
84. Das, M.; Ray, P.G.; Dhara, S.; Roy, S. Symbiotically Augmented removal of Congo red by polyaniline/cobalt sulfide/graphite composites. *Mater. Chem. Phys.* **2022**, *278*, 125487. [CrossRef]
85. He, X.Y.; Gan, J.G.; Fakhri, A.; Dizaji, B.F.; Azarbaijan, M.H.; Hosseini, M. Preparation of ceric oxide and cobalt sulfide-ceric oxide/cellulose-chitosan nanocomposites as a novel catalyst for efficient photocatalysis and antimicrobial study. *Int. J. Biol. Macromol.* **2020**, *143*, 952–957. [CrossRef]